

Supporting information

Reduction of Cr(VI) by Synergistic Effects of Iron-Rich Biochar and *Pseudomonas aeruginosa*

Bei Ou¹, Hui Wang¹, Keke Xiao*, Yuwei Zhu, Yuan Liu, Sha Liang, Huijie Hou,
Wenbo Yu, Jingping Hu, Jiakuan Yang

*School of Environmental Science and Engineering, Huazhong University of Science
and Technology, 1037 Luoyu Road, Wuhan, Hubei, 430074, China*

¹These two authors contributed equally to this manuscript.

* Corresponding author. Tel.: +86 27 87540995; Fax: +86 27 87792207.

E-mail address: xiaokeke@hust.edu.cn (K. K. Xiao)

Contents

Text S1. Iron-Based Biochar Preparation	1
Text S2. Testing and Characterization Methods	2
Table S1. Main characteristics of raw sludge.	5
Table S2. Chemical composition of culture medium.....	6
Table S3. Phosphorus species in the aqueous and solid phase.	7
Table S4. The comparison of the reduction of Cr(VI) with other studies.	8
Figure S1. The schematic of this study.....	9
Figure S2. The growth curve of PA.....	10
Figure S3. Effect of Cr(VI) concentration on the growth of PA.	11
Figure S4. Interaction effects of PA and biochar.	12
Figure S5. The effect of protein extracts from various cellular components on reducing Cr(VI).	13
Figure S6. Fe 2p XPS profiling spectra of (a) Fe-300 and (b) Fe-800 at the pyrolysis temperatures of 300 °C and 800 °C, respectively.	14
Figure S7. (a) The picture shows the reaction of Cr(VI) and Fe(II) and (b) the changes of Cr(VI) concentration in Fe-300, Fe-800, Cr + Fe-300 and Cr + Fe-800 groups as the incubation process proceeded.....	15
Figure S8. The EDS of (a) PA, (b) Fe-300, (c) Fe-300 + PA, (d) Cr + Fe-300 and (e) Cr + Fe-300 + PA.	16
Figure S9. The determination of phosphorus species in the liquid phase.....	17

Text S1. Iron-Based Biochar Preparation

Firstly, the raw sludge sample needed to be conditioned with Fenton's reagent under laboratory conditions, and then was dewatered with a diaphragm filter press. The dose of Fenton's reagent was based on the previous optimization results, with the dose of Fe^{2+} was 110 mg/g VS, and the dose of H_2O_2 was 88 mg/g VS [61]. For the raw sludge, without adding any reagents, it was directly dewatered through the plate frame. Subsequently, both these two sludge samples were dewatered using a laboratory-scale diaphragm filter press [30]. When the whole dewatering was over, the mud cake was taken out and dried in a blast drying oven at 105 °C. Samples was crushed, grinded, sieved (80 mesh), and sealed for storage in order at last.

Using a horizontal tubular pyrolysis furnace for pyrolysis biochar, sludge was loaded into a porcelain combustion boat and placed in the furnace with an inert atmosphere (argon gas, purity of 99.99%) for 10 - 20 min and the carrier gas flow rate of 100 mL/min to ensure that the entire pyrolysis environment was anaerobic. The program was restarted at a heating rate of 10 °C/min until reach the target temperature which was kept for 2 h. When the pyrolysis was completed, take out samples after the furnace cooling to ambient temperature and save them for later use.

Text S2. Testing and Characterization Methods

The total chromium concentration was measured by inductively coupled plasma optical emission spectrometer (ICP-OES) (Optima8300DV, Perkin Elmer, America). Solid sample of a certain mass was weighted accurately to 0.001 g and digested it with HClO₄-HNO₃-HF [62]. After digestion, the sample was selected a 0.45 μm microporous membrane for filtration, stored at -4 °C refrigerator, and then determined by ICP-OES. Single-element standard solution was adopted in national standard sample for standard curve of each element with diluting to the preset concentration gradient. The concentration of Cr(VI) was analyzed by 1,5 diphenylcarbazide spectrophotometric method [63]. The concentration of Cr(III) was obtained from the concentration difference between total chromium and Cr(VI). To investigate interaction effects (E) between *Pseudomonas aeruginosa* (PA) and biochar in the reduction of Cr(VI), interaction effects (synergistic, antagonism and independent effects) were calculated through the formula: $E = \{[A - \max(B, C)]/A\}$, corresponding to $E > 0$ as the synergistic effect [64]. Here A, B, and C were the Cr(VI) removal efficiencies in Cr + Fe-800 + PA (or Cr + Fe-300 + PA), Cr + PA and Cr + Fe-800 (or Cr + Fe-300).

The determination of phosphorus in the aqueous phase is shown in Figure S9 (Supporting Information). The analytical method of phosphorus species in the solid sample was in accordance with Hedley's method [65]. Solid sample to determine total phosphorus content in solid phase was extracted by burning, 0.2 g of which was weighed and burned in a muffle furnace at 600 °C for 2 h. Leached with 1 mol/L HCl,

the sample mixture was heated at 25 °C, 150 revolutions per minute (rpm) shaking for 16 h. Through centrifugal separation, samples were determined by ammonium molybdate spectrophotometry. The specific processes of phosphorus forms in solid samples were described briefly below. 0.1 ± 0.001 g solid sample was placed in a 50 mL tube which was added with 20 mL extractant in order, including H₂O (H₂O-P), 0.5 mol/L NaHCO₃ (NaHCO₃-P), 0.1 mol/L NaOH (NaOH-P) and 1 mol/L HCl (HCl-P) at a constant temperature shaking for 16 h, then centrifuged for solid-liquid separation. Digested with potassium persulfate, the liquid was determined by ammonium molybdate spectrophotometry. As for the obtained solid residue after the above four-step extraction, it was freeze-dried, then placed in a muffle furnace for calcination at 600 °C for 4 h. Leaching with 1 mol/L HCl, the mixture was shaken at 25 °C, 150 r/min for 16 h and centrifuged to be determined by ammonium molybdate spectrophotometry.

The concentrations of Fe(II) and total Fe in the aqueous phase were determined using the 1,10-phenanthroline method at 510 nm by a UV-1800 spectrophotometer (Shimadzu, Japan), according to methods described in Schnell et al. [66]. The concentration of Fe(III) was calculated by subtracting the Fe(II) concentration from the total iron concentration.

The binding states of Fe on the surface of the Fe biochar were analyzed using X-ray photoelectron spectroscopy (XPS) (PHI-5300/ESCA, Kyoto, Japan). The detailed profiles of Fe oxidation states (Fe(III), Fe(II), and Fe(0)) were characterized as described in Xu et al. [67]. Briefly, the qualitative determination of Fe oxidation

states was conducted based on the specific peak positions of different iron species (Fe 2p_{3/2} peak positions for Fe(III), Fe(II), and Fe(0) are 711.2, 709.2, and 706.7 eV, respectively; Fe 2p_{1/2} peak positions for Fe(III), Fe(II), and Fe(0) are 724.8, 722.8, and 719.8 eV, respectively; the satellite peak positions for Fe(III) are 718.9 and 733.4 eV, and for Fe(II) are 714.6 and 729.5 eV, respectively). The Fe 2p XPS spectra were deconvoluted into the Fe(0), Fe(II), and Fe(III) peaks.

Table S1. Main characteristics of raw sludge.

Moisture content*	pH*	TS*	VS*	TP*	PO ₄ ³⁻ -P*	ORP*
(%)		(g/L)	(g/L)	(mg/L)	(mg/L)	(mV)
98.1	6.72	19.1	10.2	188.1	172.4	-260.0
± 0.01	± 0.01	± 0.09	± 0.07	± 3.20	± 2.65	± 15.24

Noted: * Mean ± SD; TS denotes total solids; VS denotes volatile solids; TP denotes total phosphorus; ORP denotes oxidation reduction potential.

Table S2. Chemical composition of culture medium.

	Chemicals	Name	Amount
Luria-Bertani liquid	C ₃ H ₅ NO	Tryptone	10 g
medium (1 L)	Yeast extract	Yeast extract	5 g
	NaCl	Sodium chloride	10 g
Mineral liquid medium*	A	Reagent A	1 L
	B	Reagent B	0.125 mL
Reagent A (1 L)	C ₇ H ₁₄ NNaO ₄ S	MOPs	10 g
	C ₃ H ₈ O ₃	Glycerol	6.5 g
	C ₄ H ₄ Na ₂ O ₄	Anhydrous disodium succinate	5 g
	NH ₄ Cl	Ammonium chloride	1 g
	KCl	Potassium chloride	0.5 g
	MgSO ₄ ·7H ₂ O	Magnesium sulfate heptahydrate	0.2 g
	CaCl ₂	Calcium chloride	0.05 g
	FeSO ₄ ·7H ₂ O	Ferrous sulfate heptahydrate	0.001 g
Reagent B (1 L)	Co(NO ₃) ₂	Cobalt nitrate	0.0065 g
	ZnSO ₄ ·7H ₂ O	Zinc sulfate heptahydrate	0.0059 g
	MnSO ₄ ·H ₂ O	Manganese sulfate monohydrate	0.005 g
	CuSO ₄ ·5H ₂ O	Copper sulfate pentahydrate	0.0036 g
	(NH ₄) ₂ MoO ₄	Ammonium molybdate	0.0029 g

Noted: * For Mineral liquid medium, only 0.125 mL of Reagent B was added into 1 L of Reagent A.

Table S3. Phosphorus species in the aqueous and solid phase.

Phases	Phosphorus species
Aqueous phase	ortho-P
	TDP
	TP
	pyro-P = TDP - ortho-P
	microbe-P = TP - TDP
Solid phase	TP
	H ₂ O-P
	NaHCO ₃ -P
	NaOH-P
	HCl-P
	residue-P

Noted: "ortho-P" means orthophosphate; "TDP" means total dissolved phosphate; "TP" means total phosphorus (TP = TDP, in the group without PA); "pyro-P " means the released pyrophosphates from the biochar; "microbe-P" means phosphorus sorbed by PA; "H₂O-P" means water soluble phosphorus; "NaHCO₃-P" means exchangeable phosphorus; "NaOH-P" means iron aluminum bound phosphorus; "HCl-P" means calcium magnesium bound phosphorus; "residue-P" means residual phosphorus

Table S4. The comparison of the reduction of Cr(VI) with other studies.

Feedstock	Pyrolysis temperature (°C)	The modification method	The dose of inocula	The initial Cr(VI) concentration	pH value	Incubation time	The removal efficiency (%)	References
Wheat straw	300 and 800	Mechanical ball milling	Biochar (1 g/L), <i>Shewanella oneidensis</i> MR-1 ($\sim 0.5 \times 10^9$ cfu/mL) and lactate (20 mmol/L)	50 mg/L	7.00	96 h	34.5 (300°C)	[68]
							48.4 (800°C)	
Wheat straw	700	-	Biochar (1 g/L), <i>Shewanella Putrefaciens</i> CN32 (1×10^8 cell/mL) and lactate (10 mM)	200 μ M	7.00	25 h	60.23 \pm 0.45	[38]
The sulfate reducing sludge	500	-	Biochar (0.5 g/L)	120 mg/L	3.00	24 h	46.93	[69]
Sludge	600	ZnO	Biochar (1 g/L)	100 mg/L	1.00	420 min	48.63	[70]
Sludge	500	nZVI	Biochar (1 g/L)	50 mg/L	7.00	90 min	59.62	[71]
Sludge	500	-	Biochar (12.5 g/L)	100 mg/L	6.00	30 d	No significant removal	[72]

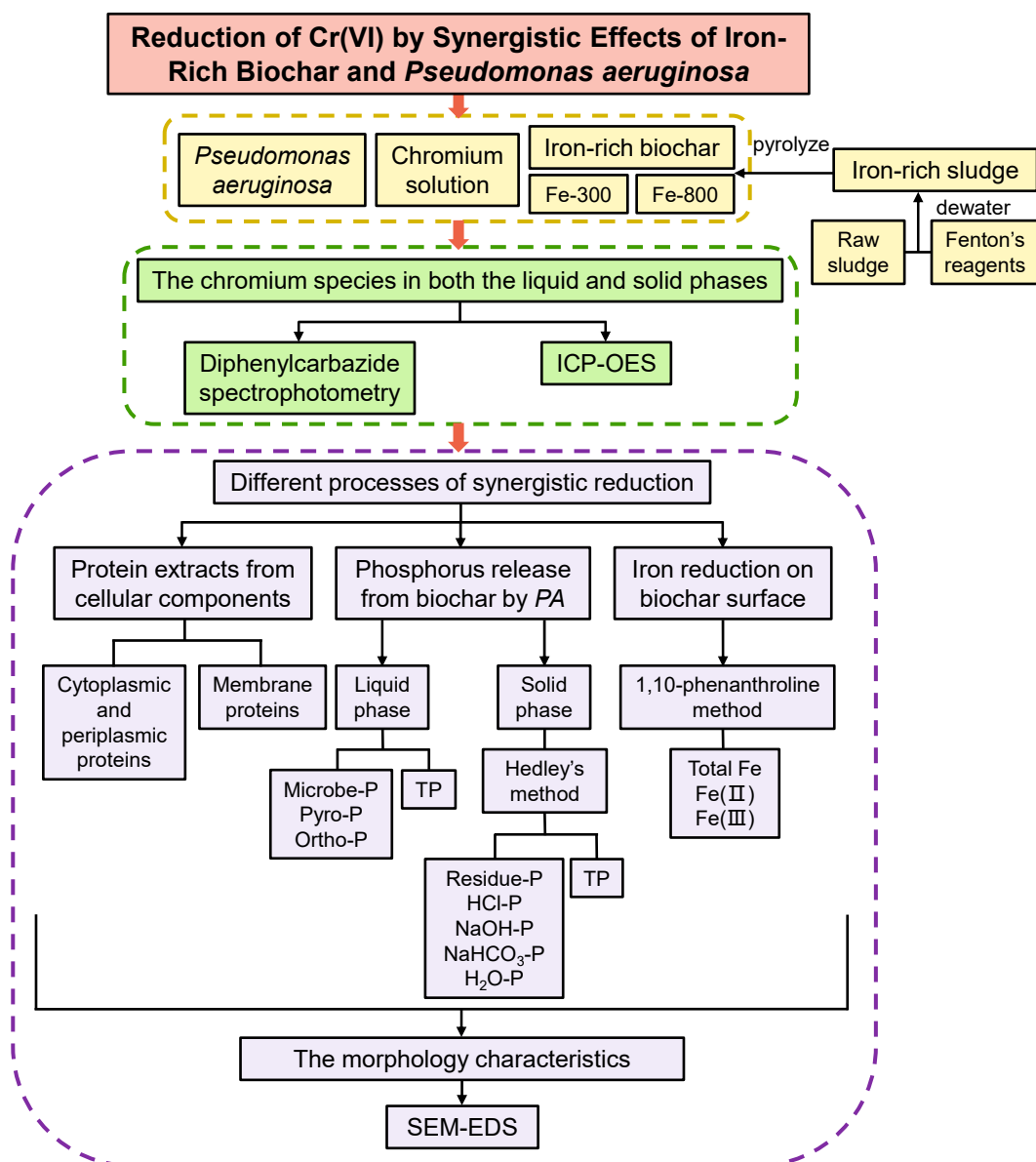


Figure S1. The schematic of this study.

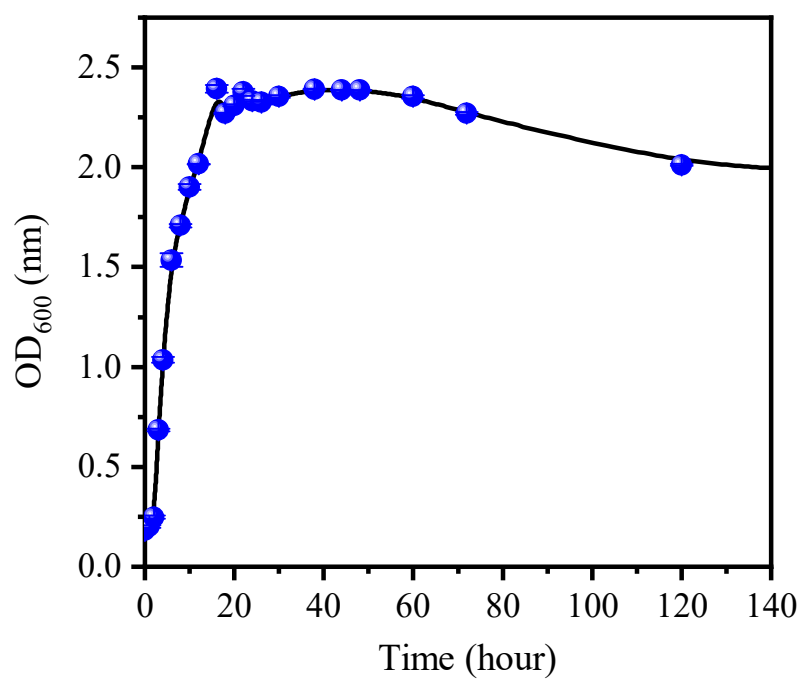


Figure S2. The growth curve of PA.

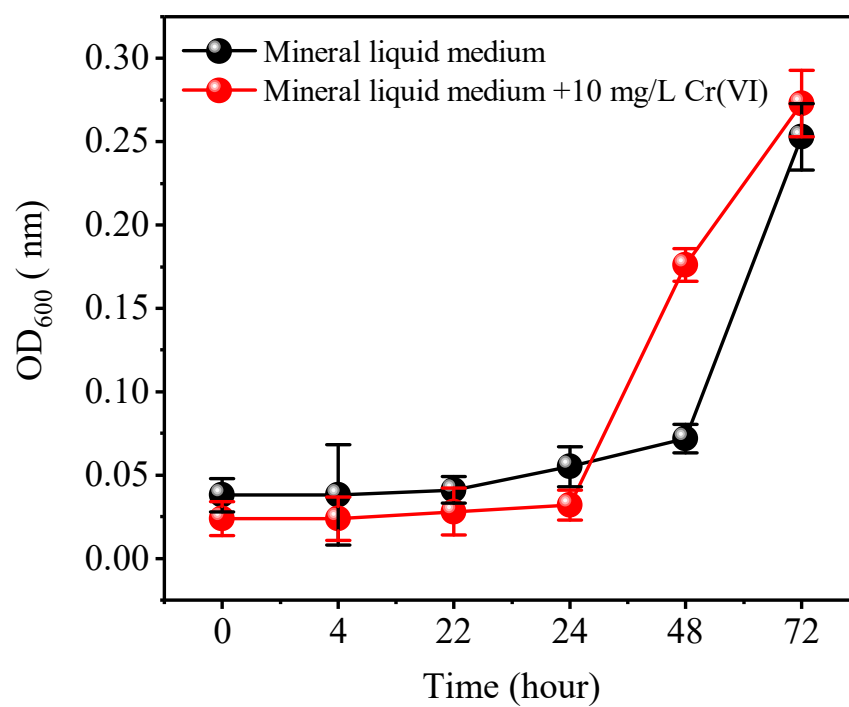


Figure S3. Effect of Cr(VI) concentration on the growth of PA.

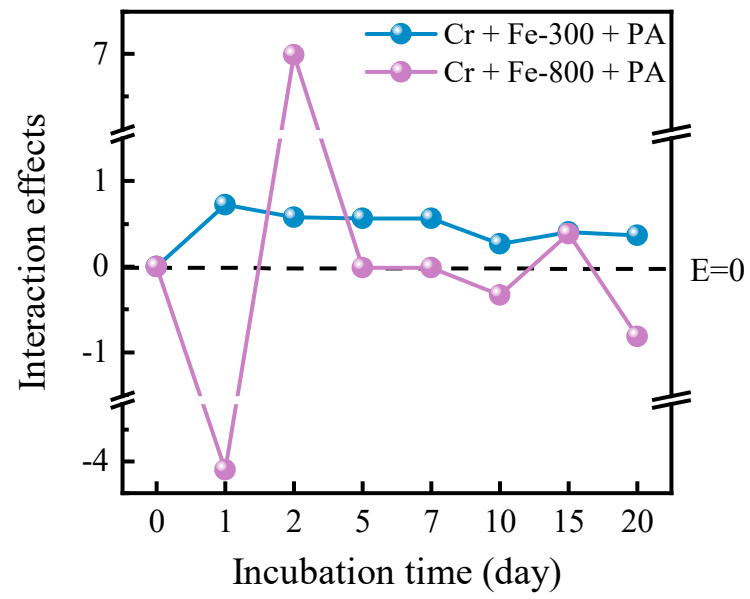


Figure S4. Interaction effects of PA and biochar.

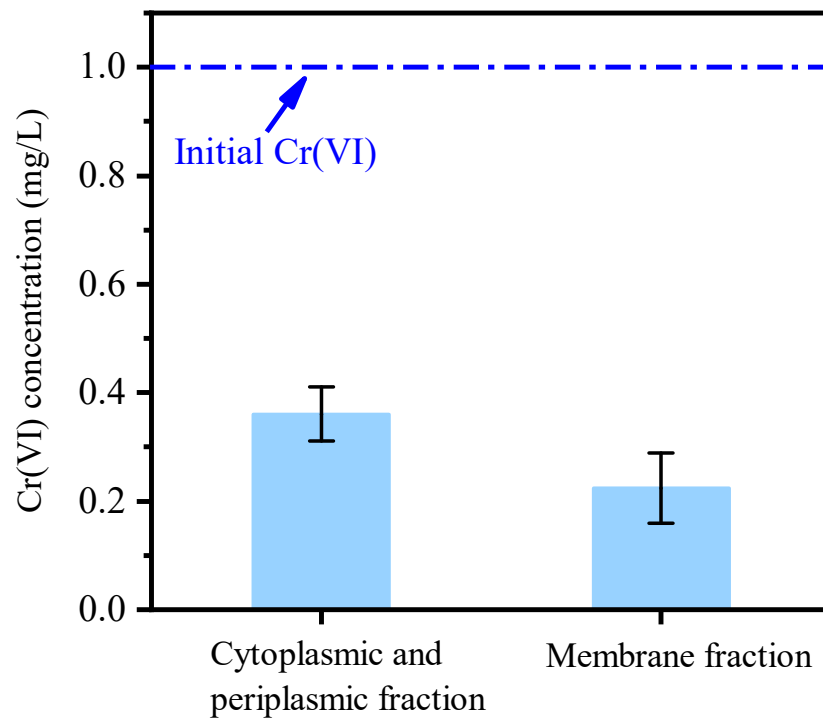


Figure S5. The effect of protein extracts from various cellular components on reducing Cr(VI).

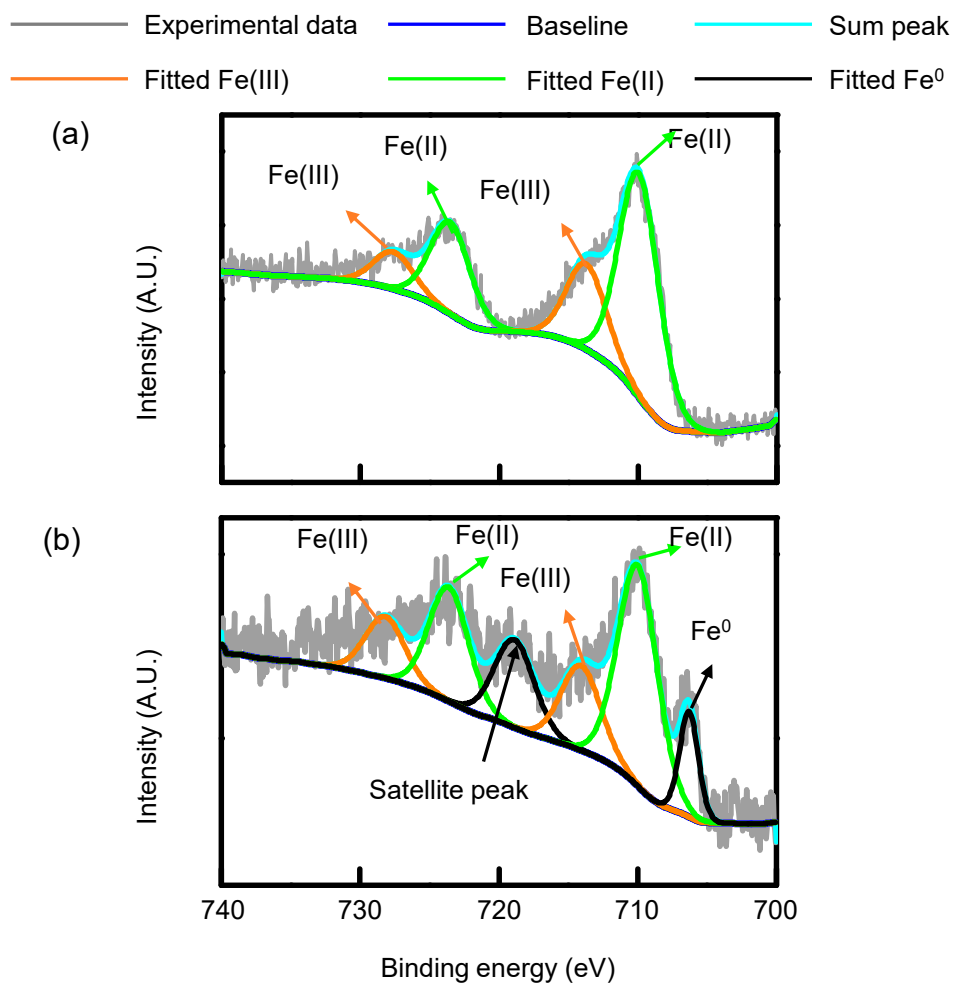


Figure S6. Fe 2p XPS profiling spectra of (a) Fe-300 and (b) Fe-800 at the pyrolysis temperatures of 300 °C and 800 °C, respectively.

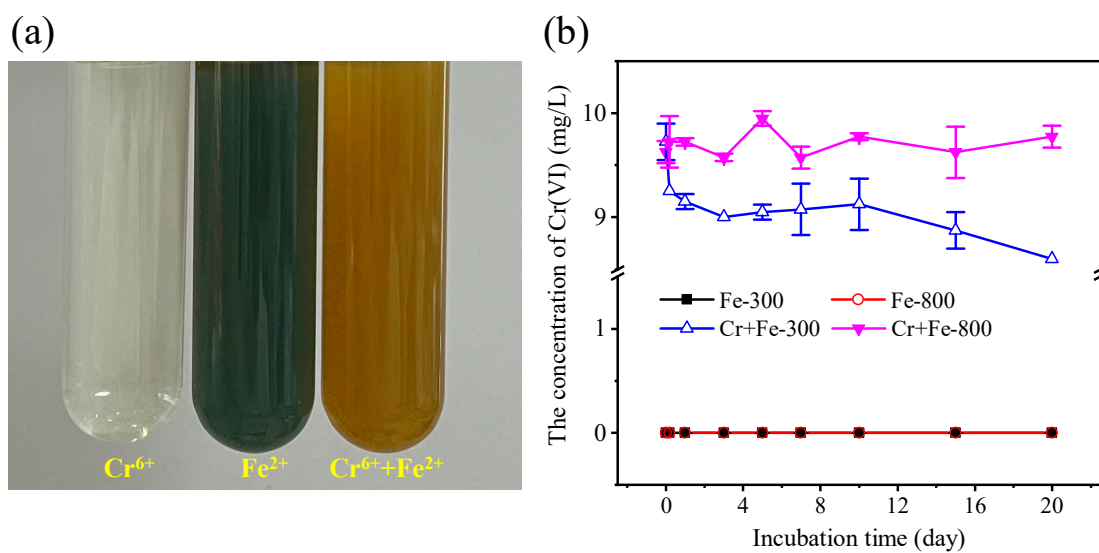


Figure S7. (a) The picture shows the reaction of Cr(VI) and Fe(II) and (b) the changes of Cr(VI) concentration in Fe-300, Fe-800, Cr + Fe-300 and Cr + Fe-800 groups as the incubation process proceeded.

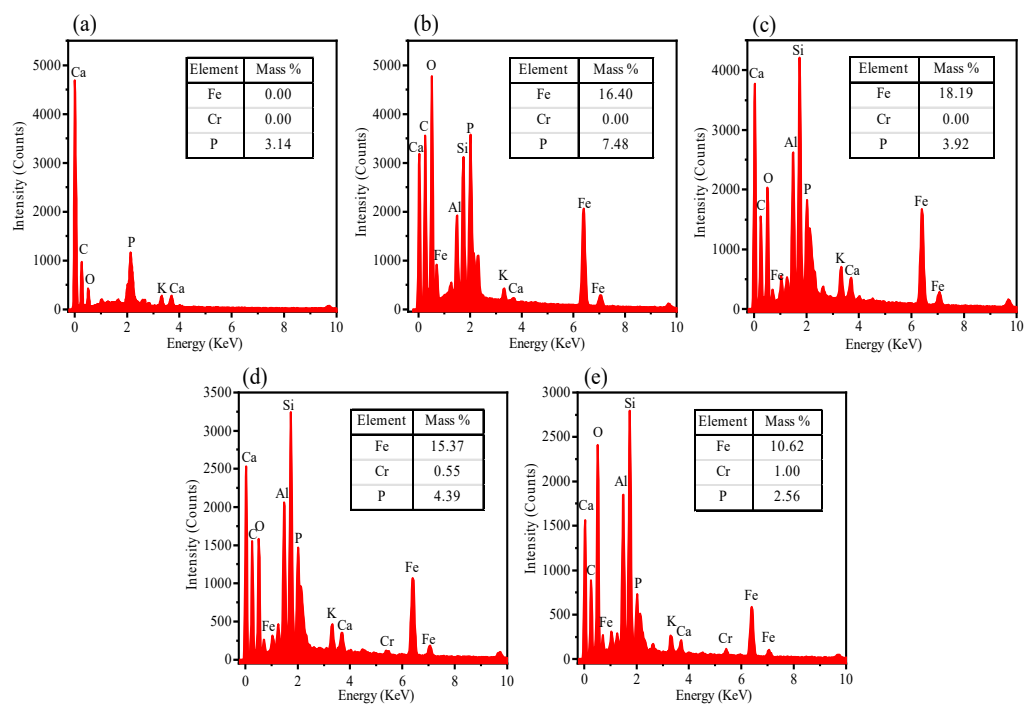


Figure S8. The EDS of (a) PA, (b) Fe-300, (c) Fe-300 + PA, (d) Cr + Fe-300 and (e)

Cr + Fe-300 + PA.

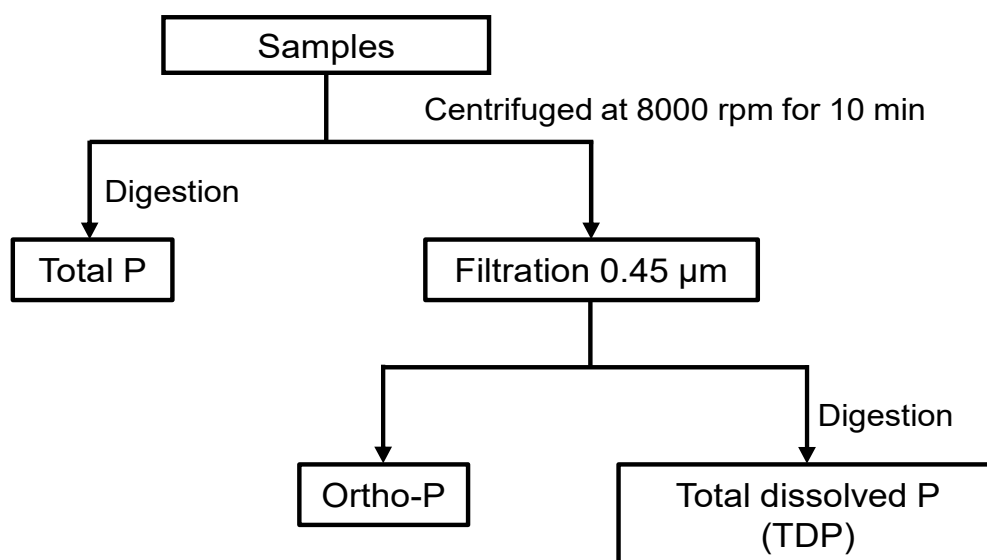


Figure S9. The determination of phosphorus species in the liquid phase.

References

30. Xiao, K.; Yu, Z.; Wang, H.; Yang, J.; Liang, S.; Hu, J.; Hou, H. and Liu, B. et al. Investigation on emission control of NO_x precursors and phosphorus reclamation during pyrolysis of ferric sludge. *Sci. Total Environ.* **2019**, 670, 932-940.
38. Zhang, B. and Jiao, W. Biochar facilitated bacterial reduction of Cr(VI) by *Shewanella Putrefaciens* CN32: Pathways and surface characteristics. *Environ. Res.* **2022**, 214(4), 113971.
61. Yu, W.; Yang, J.; Tao, S.; Shi, Y.; Yu, J.; Lv, Y.; Liang, S.; Xiao, K.; Liu, B.; Hou, H.; Hu, J. and Wu, X. A comparatively optimization of dosages of oxidation agents based on volatile solids and dry solids content in dewatering of sewage sludge. *Water Res.* **2017**, 126, 342-350.
62. Kim, S. O.; Moon, S. H.; Kim, K. W. and Yun, S. T. Pilot scale study on the ex-situ electrokinetic removal of heavy metals from municipal wastewater sludges. *Water Res.* **2002**, 36, (19), 4765-4774.
63. USEPA. 1992. Method 7196A: Chromium, Hexavalent (Colorimetric).
64. Yu, Y.; An, Q.; Zhou, Y.; Deng S.; Miao, Y.; Zhao, B. and Yang, L. Highly synergistic effects on ammonium removal by the co-system of *Pseudomonas stutzeri* XL-2 and modified walnut shell biochar. *Bioresour. Technol.* **2019**, 280, 239-246.
65. Hedley, M.; Stewart, J. and Chauhan, B. Changes in inorganic and organic soil phosphorus fractions induced by cultivation practices and by laboratory incubations. *Soil Sci. Soc. Am. J.* **1982**, 46(5), 970-976.

66. Schnell, S.; Ratering, S. and Jansen, K. Simultaneous determination of iron(III), iron(II), and manganese(II) in environmental samples by ion chromatography. *Environ. Sci. Technol.* **1998**, 32.
67. Xu, H.; Sun, Y.; Li, J.; Li, F. and Guan, X. Aging of zerovalent iron in synthetic groundwater: X-ray photoelectron spectroscopy depth profiling characterization and cepassivation with uniform magnetic field. *Environ. Sci. Technol.* **2016**, 50(15), 8214-8222.
68. Ri, C.; Tang, J.; Liu, F.; Lyu, H. and Li, F. Enhanced microbial reduction of aqueous hexavalent chromium by *Shewanella oneidensis* MR-1 with biochar as electron shuttle. *J. Environ. Sci.* **2022**, 113, 12-25.
69. Ma, R.; Yan, X.; Pu, X. and Fu, X. An exploratory study on the aqueous Cr(VI) removal by the sulfate reducing sludge-based biochar. *Sep. Purif. Technol.* **2021**, 276(10) , 119314.
70. Zhao, X.; Feng, H.; Jia, P.; An, Q. and Ma, M. Removal of Cr(VI) from aqueous solution by a novel ZnO-sludge biochar composite. *Environ. Sci. Pollut. Res. Int.* **2022**, 29(55), 83045-83059.
71. Chen, X.; Fan, G.; Li, H.; Li, Y.; Zhang, R.; Huang, Y. and Xu, X. Nanoscale zero-valent iron particles supported on sludge-based biochar for the removal of chromium (VI) from aqueous system. *Environ. Sci. Pollut. Res. Int.* **2022**, 29(3), 3853-3863.
72. Fei, Y.; Li, M.; Ye, Z.; Guan, J.; Huang, Z.; Xiao, T. and Zhang, P. The pH-sensitive sorption governed reduction of Cr(VI) by sludge derived biochar

and the accelerating effect of organic acids. *J. Hazard. Mater.* **2022**,
423(B):127205.